AGU ADVANCING EARTH AND SPACE SCIENCE

Geophysical Research Letters

RESEARCH LETTER
10.1029/2021GL096590

Historical Rankings and Vortices' Activities of the Extreme Mei-yu Seasons: Contrast 2020 to Previous Mei-yu Seasons

Shen-Ming Fu[1], Huan Tang[2,3], Jian-Hua Sun[2], Tian-Bao Zhao[4], and Wan-Li Li[5]

[1]International Center for Climate and Environment Sciences, Institute of Atmospheric Physics, Chinese Academy of Sciences, Beijing, China, [2]Laboratory of Cloud–Precipitation Physics and Severe Storms, Institute of Atmospheric Physics, Chinese Academy of Sciences, Beijing, China, [3]University of Chinese Academy of Sciences, Beijing, China, [4]Key Laboratory of Regional Climate-Environment Research for East Asia, Institute of Atmospheric Physics, Chinese Academy of Sciences, Beijing, China, [5]China Meteorological Administration Training Center, Beijing, China

Key Points:

- Historical rankings of the precipitation within different regions during extreme Mei-yu seasons were determined for the first time
- Quantitative contributions of mesoscale vortices to the total precipitation of the extreme Mei-yu seasons were shown for the first time
- Abnormally active vortices in the 2020 Mei-yu season were the direct reason for its abnormally high rainfall within/around Sichuan Basin

Supporting Information:

Supporting Information may be found in the online version of this article.

Correspondence to:

S.-M. Fu,
fusm@mail.iap.ac.cn

Citation:

Fu, S.-M., Tang, H., Sun, J.-H., Zhao, T.-B., & Li, W.-L. (2022). Historical rankings and vortices' activities of the extreme Mei-yu seasons: Contrast 2020 to previous Mei-yu seasons. *Geophysical Research Letters*, *49*, e2021GL096590. https://doi.org/10.1029/2021GL096590

Received 12 OCT 2021
Accepted 22 DEC 2021

Author Contributions:

Conceptualization: Shen-Ming Fu
Data curation: Shen-Ming Fu, Huan Tang, Tian-Bao Zhao
Formal analysis: Shen-Ming Fu, Huan Tang
Funding acquisition: Shen-Ming Fu
Investigation: Shen-Ming Fu
Methodology: Shen-Ming Fu, Huan Tang
Project Administration: Shen-Ming Fu, Jian-Hua Sun
Resources: Shen-Ming Fu, Huan Tang, Jian-Hua Sun
Software: Shen-Ming Fu, Huan Tang
Supervision: Shen-Ming Fu, Jian-Hua Sun, Tian-Bao Zhao, Wan-Li Li
Validation: Shen-Ming Fu, Huan Tang, Jian-Hua Sun
Visualization: Shen-Ming Fu
Writing – original draft: Shen-Ming Fu
Writing – review & editing: Shen-Ming Fu

Abstract

The Mei-yu season (MYS) is one of the most important components of the East Asian rainy season. As the MYS rainfall is significantly uneven, determining its notable features is crucial to understanding/predicting the MYS precipitation. This study provided the first report on the historical rankings of the accumulated precipitation within different regions during extreme MYSs. It was shown that, in the extreme 2020 MYS, the area-averaged precipitation within/around the Sichuan Basin ranked first during a 70-year period. For the first time, quantitative contributions of mesoscale vortices to the total precipitation of extreme MYSs were shown. It was found that, during the 2020 MYS, vortices accounted for up to 50% of the MYS's duration within/around Sichuan Basin, and induced up to 90% of the total precipitation there. The abnormally active vortices in the 2020 MYS were the direct reason for the highest precipitation in the past 70 years within/around the Sichuan Basin.

Plain Language Summary

The Mei-yu season (MYS) is a climatic phenomenon of continuous overcast and rainy weather (typically appears in June and July), that occurs in the Yangtze River Basin, Taiwan, Japan and Southern Korea. As the MYS rainfall was uneven, to determine its notable features is crucial to understanding and predicting the MYS precipitation. We provided the first report on the historical rankings of the accumulated precipitation within different regions during the extreme MYSs of 1954, 1998 and 2020. It is shown that, during the 2020 MYS, the area-averaged precipitation within/around Sichuan Basin was the highest in the past 70 years. By calculating the quantitative contributions of mesoscale vortices to the total MYS precipitation (this study provided the first report), we attributed the abnormally high precipitation within/around Sichuan Basin of the 2020 MYS to the abnormally active mesoscale vortices in this region. Results show that, during the 2020 MYS, vortices accounted for up to 50% of the MYS's whole duration within/around Sichuan Basin, and induced up to 90% of the total precipitation there. Therefore, improving the forecast of mesoscale vortices is of great importance to improve the MYS-rainfall prediction.

1. Introduction

In Asia, China suffers the most severe flood-related economic loss, with an annual mean direct economic loss of ~250 billion RMB (Song, 2018). Of these, a large proportion appeared in the Yangtze River Basin (YRB), due to torrential rainfall events in the Mei-yu season (MYS) (Tao 1980; Zhao et al., 2004). The MYS (also known as Changma in Korea and Baiu in Japan), which typically persists from early June to mid-July, is one of the most important components of the East Asian rainy season (Tao & Chen, 1987; Tanaka, 1992; Oh et al., 1997). A quasistationary front (known as the Mei-yu front), resulted from the encountering of the warm-wet air from the tropics and cold-dry air from middle-high latitudes, is the most significant feature of the MYS (Fu et al., 2018; Ninomiya, 2000; Zhao et al., 2004). This front has dual effects on the precipitation in the MYS: on the one hand, it directly induces precipitation, and on the other hand, it favors formation and sustainment of meso (2–2,000 km), and/or small-scale (smaller than 2 km) systems (Orlanski, 1975), particularly the mesoscale vortices, which usually induced more persistent and intense precipitation (Dong & Zhao, 2004; Fu et al., 2013, 2016; Zhang et al., 2004).

The YRB experienced ~18 severe floods during the 20th century, most of which appeared in the MYS (Zong & Chen, 2000). Of these, the 1954 flood with more than 33,000 people killed and ~4.3 million home demolished, and the 1998 flood with 1,320 casualties and ~5 million destroyed homes, were the most devastating floods (Wei et al., 2020; Zong & Chen, 2000). Entering the 21st century, floods are still active over the YRB (e.g., 2003, 2007, 2010, 2016), with the most severe one appeared in the 2020 MYS (Liu et al., 2021; Lu & Takaya, 2021; Wei et al., 2020). In terms of duration, the 2020 MYS was about twice of the climatology (Ding et al., 2021), and in terms of the accumulated rainfall, it set the highest record since 1961 (Qiao et al., 2021). Overall, the severe floods during the 2020 MYS affected ~45.5 million people and caused a direct economic loss of more than 170 billion RMB (Ye & Qian, 2021), making it one of the most influential disastrous events in 2020 (Japan Meteorological Agency, 2020; Park et al., 2021; Wei et al., 2020).

Due to its great importance, tremendous efforts had been made to explore the key features, possible formation mechanisms, and prediction skills of the record-breaking 2020 MYS (Bett et al., 2021; Chen et al., 2021; Clark et al., 2021; Ding et al., 2021; Qiao et al., 2021; Volonté et al., 2021; Wang et al., 2021; Wei et al., 2020; Ye & Qian, 2021; Zhao et al., 2021). However, after a series of studies, two crucial scientific issues still remained unsolved: (a) As precipitation of MYSs was notably uneven, there lacked the spatial evaluations of the 2020 Mei-yu rainfall within different regions of the YRB. This is vital to reach a more comprehensive understanding of the extreme 2020 MYS, and to ascertain its most notable feature. (b) Although mesoscale vortices had long been confirmed to frequently induce torrential rainfall events during the MYSs, no previous studies had shown their quantitative contributions. To evaluate the contributions of the mesoscale vortices to the extreme 2020 MYS is useful to enhance the understanding of the Mei-yu rainfall and to adjust related prediction methods.

2. Data and Method

The daily precipitation observations at 111 stations (Figures 1a and 1b) were used to evaluate the precipitation within different regions of the YRB during 70 MYSs (from 1951 to 2020; Figure S1 in Supporting Information S1). Precipitation observations at all the 111 stations had undergone strict quality control (http://data.cma.cn/data/detail/dataCode/A.0012.0001.html), and their missing rates were 0 during the study period. Four $6° \times 8°$ boxes divided the Mei-yu rainfall region into 4 areas (Figure 1a). These were defined as Area 1–4 (A1–4), with 20 (one station every ~160 km on average) to 32 (one station every ~120 km) stations located within them, respectively. According to the regional division of the YRB, A1 (which was mainly located over the eastern section of the Tibetan Plateau; Figure S2 in Supporting Information S1) and A2 (which mainly contained the Sichuan Basin; Figure S2 in Supporting Information S1) mainly covered its upper reaches, and A3 and A4 mainly covered its middle and lower reaches, respectively. As discussed in the introduction, the MYSs in 1954, 1998, and 2020 are the most severe MYSs in recent 70 years, with their main precipitation period primarily appeared in June and July (Qiao et al., 2021; Sun & Zhao, 2003; Tao, 1980). Therefore, June and July were used to represent the extreme MYSs of 1954, 1998 and 2020.

Mesoscale vortices that affect the YRB can be roughly divided into the Tibetan Plateau vortex (TPV) (Curio et al., 2019), southwest vortex (SWV; Fu et al., 2015), and Dabie vortex (DBV) (Fu et al., 2016; Zhang et al., 2015). This study regarded a closed counterclockwise circulation in the stream field coupled with a cyclonic-vorticity center $\geq 10^{-5}$ s^{-1} as a mesoscale vortex (Fu et al., 2020). According to the central level of different vortices (Curio et al., 2019; Fu et al., 2016; Zhang et al., 2015), 500 hPa, 700 hPa, and 850 hPa were used to detect TPVs, SWVs, and DBVs, respectively (Figure S3 in Supporting Information S1). The hourly $0.25° \times 0.25°$ ERA5 reanalysis data from the European Center for Medium Range Weather Forecasts (Hersbach et al., 2020) was utilized to detect vortices using the high-accuracy identifying method developed by Fu et al. (2020). All detected vortices had undergone manual check to remove errors during the algorithm identification. The station observed precipitation (i.e., hourly precipitation observations at 2,411 stations over China) appeared within 300 km (which was close to the typical horizontal scale of the three types of vortices) from a vortex's center was regarded as associated with it. As the ERA5 reanalysis data from 1979 onwards was the final release, but that for 1950–1978 was a preliminary back extension (https://cds.climate.copernicus.eu/cdsapp#!/dataset/reanalysis-era5-pressure-levels?tab=overview), we only compared mesoscale vortices during the extreme MYSs of 1998 and 2020.

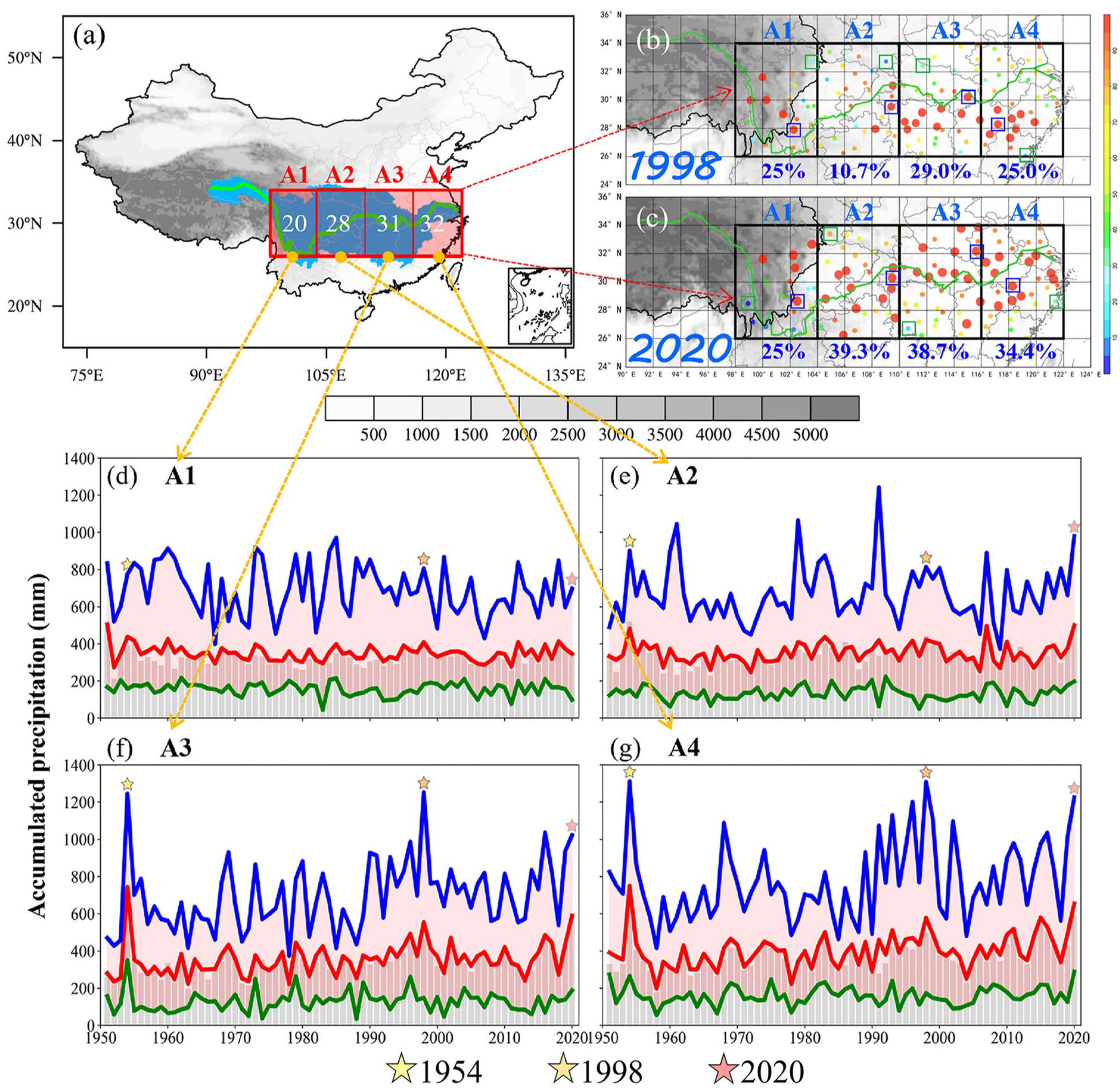

Figure 1. Panel (a) shows the range of Yangtze River Basin (blue shading), the four areas (A1–A4), and the station numbers within each area (white numbers). Panels (b–c) show the percentiles of the Mei-yu season (MYS)-accumulated precipitation at every station within A1–A4 (shading dots), where big dots mean that the accumulated precipitation exceeds the 95th percentile (during the 70-year period), small blue and green boxes mark the locations of the maximum and minimum accumulated precipitation, respectively, and blue numbers show the percentage of stations within A1–A4 (relative to all stations in A1–A4, respectively) that have a MYS-accumulated precipitation exceeding their 95th percentiles. Panels (d–g) show the 70-year time series of MYS-accumulated precipitation within A1–A4, respectively, where the blue, red, green lines show the maximum, mean, and minimum accumulated precipitation within each area, respectively, and the gray bar show the median accumulated precipitation within each area.

3. Historical Ranking

During the 70-year period from 1951 to 2020, on average, the MYS-accumulated precipitation increased from A1 (347 mm) to A4 (402 mm; Table 1), corresponding to the distribution of the eastward increasing specific humidity (the YRB borders the sea in the east; Figure 1a). Overall, variances of the time series of the maximum, average, median and minimum of the MYS accumulated precipitation all tended to increase eastward (Figures 1d–1g), implying that interannual differences of the MYS precipitation became larger from west to east. In the 70-year period, the time series of the maximum, average, median and minimum of the MYS accumulated precipitation within A1–A4 all showed no significant linear trends (not shown).

Table 1
The Maximum/Average/Median of the MYS-Accumulated Precipitation (Units: mm) and Their Ranking in the 70-Year Period Within Key Areas A1–A4, Respectively, Where the Values in the First Column Show the 70-Year A1–A4 Averaged Accumulated Precipitation (Units: mm), Respectively

Region	Year	Average	Ranking	Maximum	Ranking	Median	Ranking
A1 (347)	1954	437	**2**	776	22	391	**3**
	1998	410	6	806	**19**	390	4
	2020	346	39	697	32	344	18
A2 (351)	1954	483	3	901	5	519	**1**
	1998	422	5	814	10	442	4
	2020	500	**1**	979	**4**	499	2
A3 (356)	1954	743	**1**	1,245	2	757	**1**
	1998	555	3	1,253	**1**	462	5
	2020	589	2	1,022	4	553	2
A4 (402)	1954	750	**1**	1,312	**1**	697	**1**
	1998	578	4	1,309	2	498	6
	2020	654	2	1,225	3	592	2

Note. The highest rankings among 1954, 1998 and 2020 are highlighted in bold.

The extreme MYSs of 1954, 1998, and 2020 were compared to the historical contemporaneous precipitation in a 70-year period to determine their rankings. In terms of the area (i.e., A1–A4 in Figure 1a, respectively) averaged precipitation, (a) for A1, 1951 ranked first (red line in Figure 1d), 1954 ranked second, 1998 ranked sixth, whereas, 2020 only ranked 39th (Table 1); (b) for A2, 1954, 1998, and 2020 were all in the top five, with the 2020 MYS ranked first and the 1954 MYS ranked third; (c) for A3, 1954, 2020, 1998, ranked first to third; and (d) for A4, 1954 and 2020 ranked first and second, respectively, and 1998 ranked fourth. In terms of the median values of precipitation, (a) for A1, 1954 (third) and 1998 (fourth) had higher rankings than that of 2020 (eighteenth; Table 1), and the first ranking appeared in 1951 (gray bar in Figure 1d); (b) for A2–A4, 1954 ranked first, 2020 ranked second, and 1998 ranked fourth to sixth (Table 1). Overall, the rankings in terms of the median values were similar to those in terms of the mean values, whereas, the rankings in terms of the maximum precipitation were notably different: (a) for A1, 1985 ranked first (blue line in Figure 1d), whereas all the three extreme MYSs ranked behind 18th (Table 1), with the highest ranking appeared in 1998 (nineteenth); (b) for A2, 1991 ranked first (Figure 1e), 2020 ranked fourth, 1954 ranked fifth and 1998 ranked tenth (Table 1); (c) for A3, 1998 and 1951 ranked first and second, respectively, and 2020 ranked fourth; and (d) for A4, 1951, 1998 and 2020 ranked first to third (Table 1).

As mentioned above, the most notable features of the 2020 MYS rainfall lay in the area-averaged precipitation within A2, A3, and A4, which ranked first, second and second in the 70-year period (Table 1). Its maximum precipitation within A4 was also notable, which ranked third. For the 1998 MYS, its most notable features lay in the maximum precipitation within A3 (ranked first) and A4 (ranked second), and the averaged precipitation within A3 (ranked third; Table 1). For the 1954 MYS, its most notable features lay in the averaged precipitation within A1–A4, and the maximum precipitation within A3 (ranked second) and A4 (ranked first; Table 1). Further contrast between the 1998 and 2020 MYSs show that, within A2–A4, more stations of the latter exceeded the 95th percentile during the 70-year period (big red dots in Figures 1b and 1c), particularly for A2, which reached up to 39.3%.

4. Activities of Mesoscale Vortices

Overall, all three types of mesoscale vortices were active during the extreme MYSs of 2020 and 1998 (Figures 2a and 2b). A total of 101 mesoscale vortices formed during the 2020 MYS (Figure 2c), slightly larger than that of 1998. Of these, the DBVs showed the least notable difference in numbers (~4% in difference), whereas their tracks and locations were significantly differed from each other (Figures 2a and 2b). The number of TPVs in the 1998 MYS was ~16% larger than that of 2020 (Figure 2c), corresponding to its much higher historical rankings of

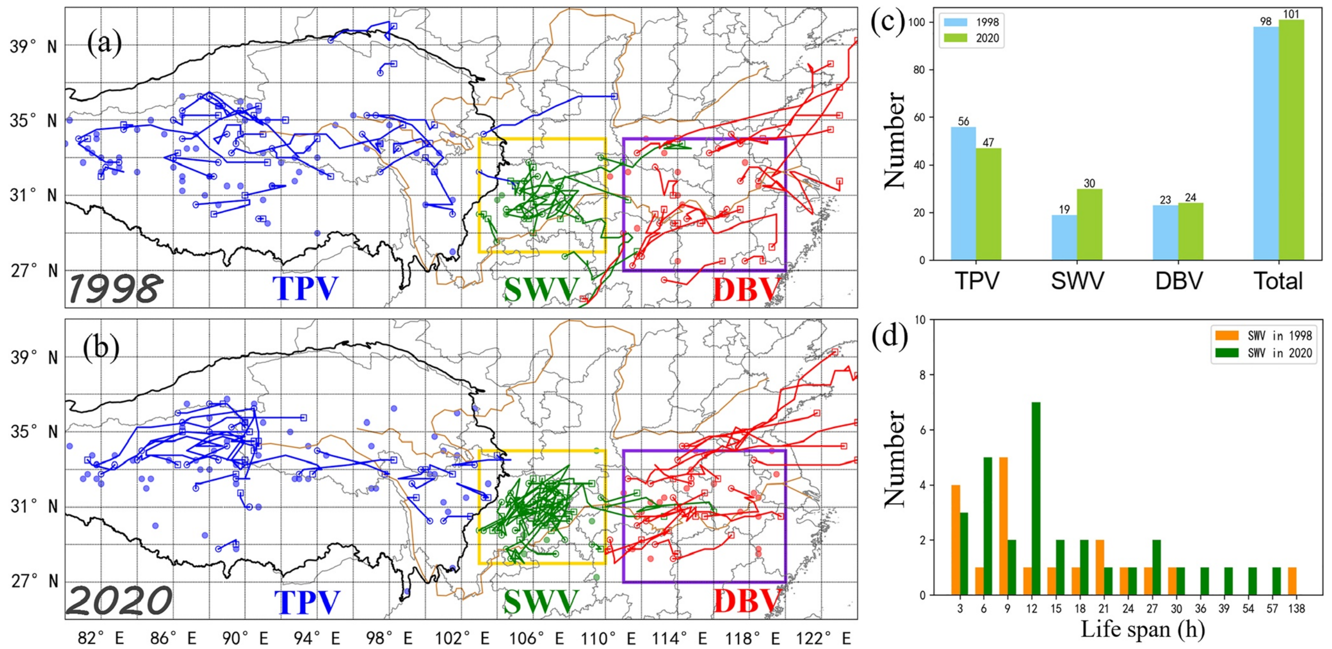

Figure 2. Panels (a–b) show the tracks of three types of mesoscale vortices in Mei-yu seasons (MYSs) of 1998 and 2020, respectively, where blue, green, and red represent the Tibetan Plateau vortex (TPV), southwest vortex (SWV), and Dabie vortex (DBV), respectively. Small open rectangles and circles mark longer-lived (≥6 hr) vortices' locations of formation and dissipation, respectively, and small shaded circles mark the shorter-lived (<6 hr) vortices' locations of formation. The curved black solid line outlines the Tibetan Plateau, the orange and purple boxes show the source regions for SWVs and DBVs, respectively. Panel (c) shows the number of TPVs, SWVs, DBVs, and their total in the MYS of 1998/2020. Panel (d) shows the number distribution of SWVs in the MYS of 1998/2020 with their life spans.

the precipitation within A1 (Table 1). The most significant difference appeared in the SWVs' numbers/lifespans (Figures 2c and 2d), with the 2020 MYS larger than that of 1998 by ∼58%/∼41%. Overall, the SWVs in both MYSs mainly showed a quasistationary behavior (in contrast, a large proportion of the other two types of vortices moved eastward/northeastward rapidly after their formation; Figures 2a and 2b), which contributed to induce persistent local heavy rainfall within A2. The above can explain why the A2-averaged precipitation during the 2020 MYS (∼42% larger in amount than climatology; Table 1) was much higher than that of 1998.

In terms of vortex-affected hours, the 2020 MYS showed similar features to those of the 1998 MYS over the western section of the Tibetan Plateau (Figures 3a and 3b), whereas within A1–A4, the two MYSs differed from each other notably. For A1, the vortex-affected hours were longer for 2020 (Figures 3a and 3b), whereas, the vortex-associated precipitation was larger for 1998 (Figures 3c and 3e). The most notable difference of the vortex-affected hours appeared in A2, with 2020 much larger than 1998 (Figures 3a and 3b). For the Sichuan Basin, which was the source for SWVs (Fu et al., 2015), mesoscale vortices appeared in around 20%–50% of the duration of the 2020 MYS (Figure 3b), but had induced up to around 30%–90% of the total accumulated precipitation (Figure 3f). These were much larger than those of 1998 (Figures 3a and 3d). Compared Figure 3d/Figure 3f with Figure 4a/Figure 4c, it can be found that, the SWVs contributed the most to the vortex-associated precipitation within A2. Therefore, the extremely excessive precipitation within A2 during the 2020 MYS (it ranked first among the 70 MYSs in terms of A2-averaged precipitation; Table 1) was mainly due to the abnormally active SWVs.

For both 1998 and 2020 MYSs, mesoscale vortices only appeared in less than 20% of the total time within A3-A4 (Figures 3a and 3b). However, their associated precipitation could contribute much larger than 20% (at some stations it was up to more than 40%) to the MYS-accumulated precipitation (Figures 3d and 3f). In addition, the maximum vortices-associated precipitation was above 1200 mm within A3 and above 1,500 mm within A4 for both MYSs (Figures 3c and 3e). These mean that the vortices-associated precipitation was strong. Compared 1998 with 2020, it can be found that, the vortices-affected hours were slightly larger for the latter (Figures 3a and 3b), and the vortices-associated precipitation amount was also slightly larger for 2020 (Figures 3c and 3e).

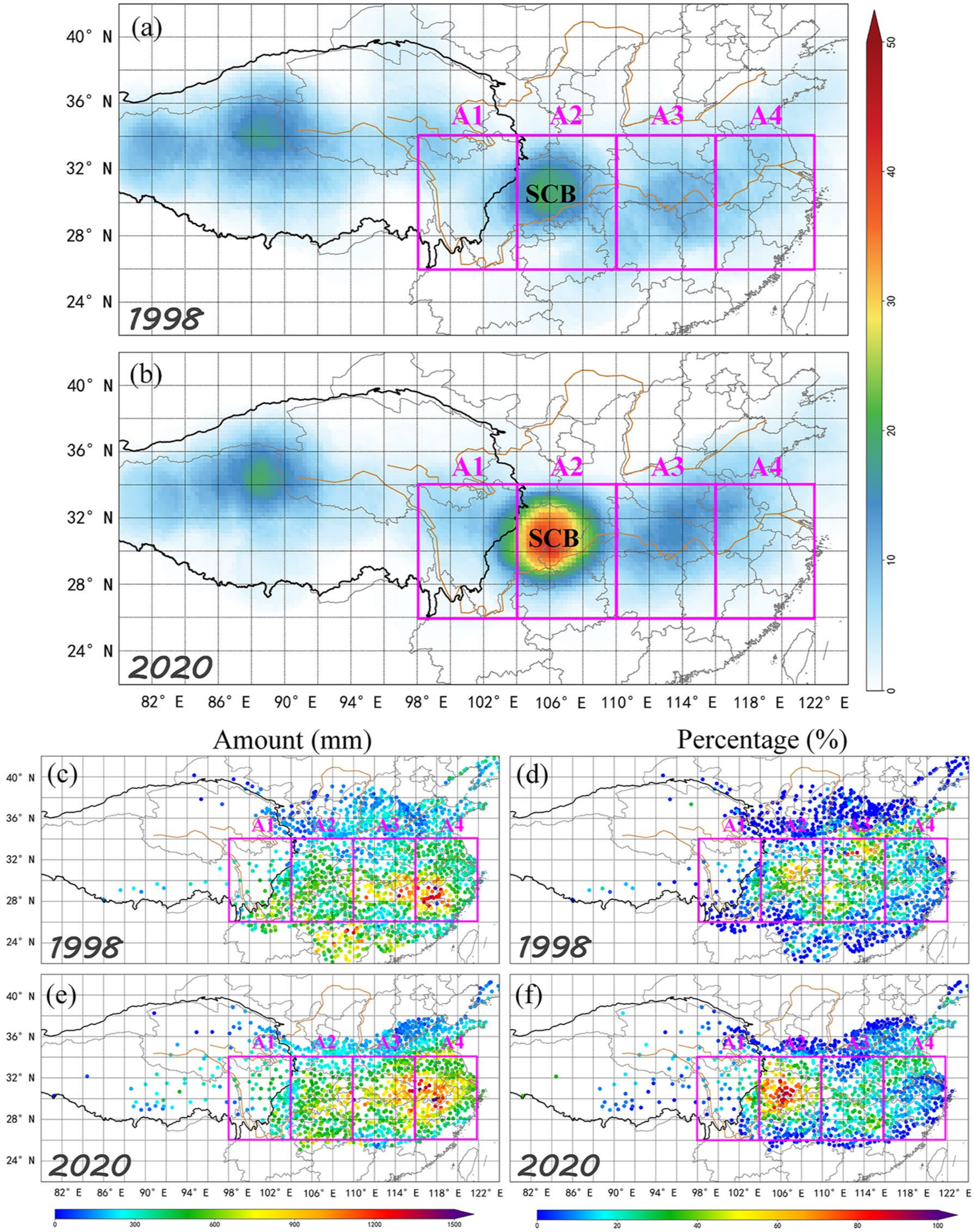

Figure 3. Panels (a–b) show the proportions (shading; %) of mesoscale-vortices-affected hours to the total Mei-yu season (MYS) duration (i.e., 1464 hr) during the MYSs of 1998 and 2020, respectively. Panels (c) illustrates the total accumulated precipitation at observational stations (shading dots; mm) associated with mesoscale vortices during the 1998 MYS. Panel (d) depicts the proportions (shading dots; %) of mesoscale-vortices-affected precipitation to the accumulated precipitation during the 1998 MYS. Panel (e) is the same as (c) but for 2020, and panel (f) is the same as (d) but for 2020. SCB = Sichuan Basin.

This was a key reason for the higher historical rankings (in terms of the averaged precipitation) of the 2020 MYS within A3-A4 (Table 1). In contrast, within A3, the vortices' contribution to the MYS-accumulated precipitation was remarkably higher for 1998 (Figures 3d and 3f), this was because that its averaged precipitation was less

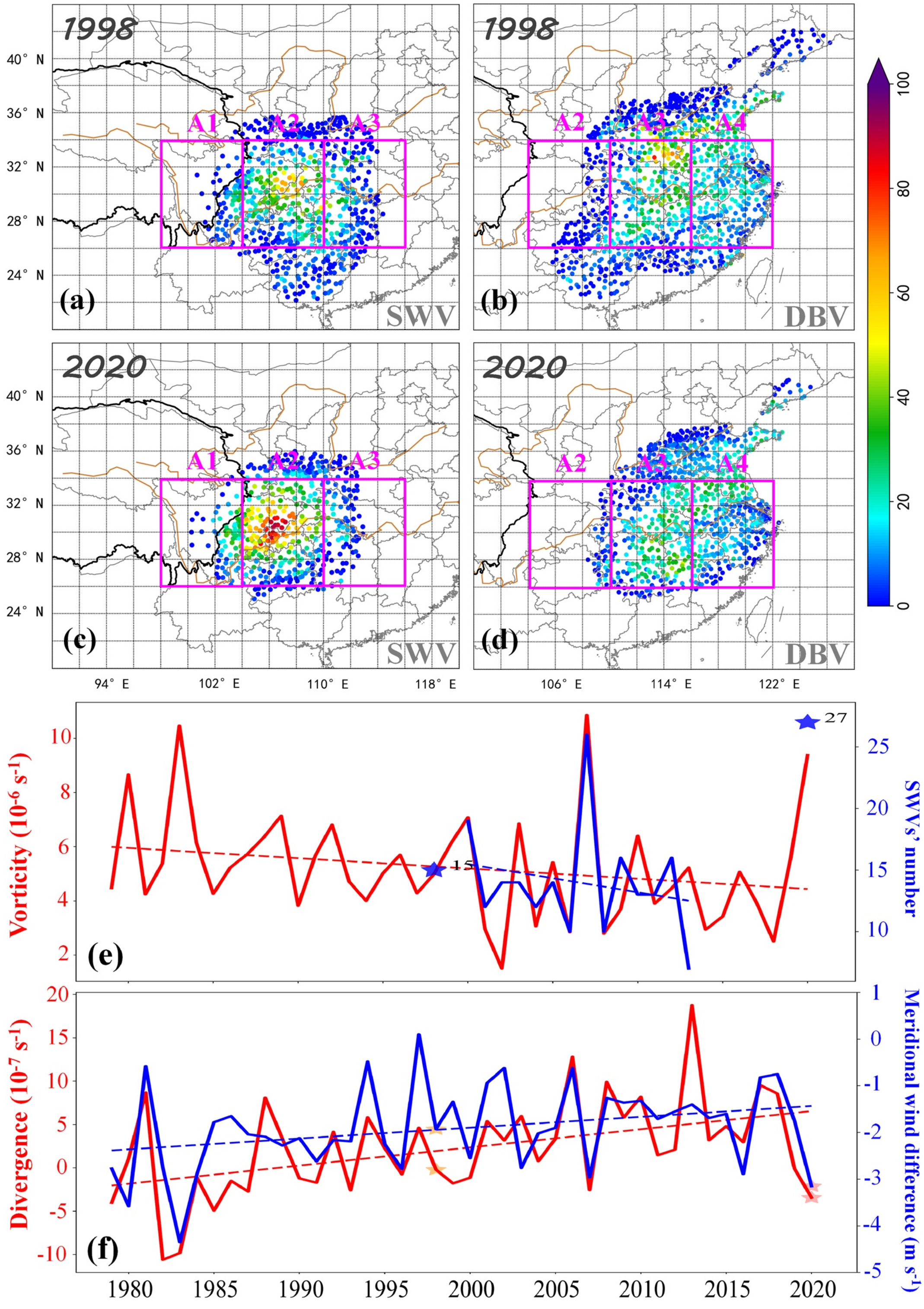

Figure 4.

than that of the 2020 MYS (Table 1). Comparison between Figures 3d and 3f with Figures 4b and 4d shows that, the DBVs made the largest contribution to the vortices-associated precipitation within A3-A4. Overall, the DBVs-associated precipitation during the 1998 MYS covered a much larger area than that of 2020 (Figures 4b and 4d), as their formation locations and tracks were more dispersed (cf., Figures 2a and 2b).

5. Possible Reasons for the Abnormally Active SWVs in 2020 MYS

As discussed in Sections 3 and 4, the highest precipitation within A2 during the past 70-year appeared in the 2020 MYS, mainly due to the SWVs. Precipitation associated with the SWVs could reach more than 900 mm at some stations within A2 (Figure 3e). Compared to that of 1998, the SWVs during the 2020 MYS showed a more focused distribution (cf., Figures 4a and 4e), which was more likely to cause flood disasters. A total of 30 SWVs appeared in the 2020 MYS, with 90% of them lasted no shorter than 6 hr (Figures 2c and 2d). Fu et al. (2015) had detected the SWVs (with a life span ≥6 hr) appeared in June and July of 2000–2013 (blue solid line in Figure 4e). Compared their results to this study it can be found that, the number of the SWVs in the 1998/2020 MYS was more than 71%/100% of the contemporaneous SWVs from 2000 to 2013 (Figure 4e). This means that the SWVs in 1998 and 2020 MYSs were more active than climatology.

Overall, the SWVs had a strong linear correlation (correlation coefficient was ~0.7 which exceeded the 99% confident level) to the A2-averaged MYS-mean vorticity (Figure 4e), as the area-averaged vorticity was an effective indicator for the vortices (Fu et al., 2017). During the 42-year period from 1979 to 2020, the averaged vorticity showed an obvious decreasing trend (Figure 4e), which exceeded the 85% confident level. This means that conditions were generally became unfavorable for producing the SWVs. It can be confirmed by the notably increasing trend of the A2-averaged MYS-mean divergence, which exceeded the 95% confident level (Figure 4f). According to the vorticity budget equation (Kirk, 2003), increasing divergence was detrimental for maintaining cyclonic vorticity (through the vertical shrinking), which was a necessary condition for the mesoscale vortices. As the A2-averaged divergence was due to the wind across the boundary lines of A2, we calculated the zonal wind difference between the western and eastern boundary lines as well as the meridional wind difference between the northern and southern boundary lines. It was found that, the meridional wind difference made a much larger proportion to the divergence than that of the zonal wind difference (not shown). Therefore, the notable increasing trend (which exceeded the 95% confident level; Figure 4f) of the meridional wind difference, which was closely related to the annual variations of summer monsoon, was the key reason for the increasing trend of the A2-averaged divergence. However, in the 2020 MYS, a situation opposite to the increasing trend of the divergence appeared: the southerly wind on the southern boundary of A2 was strong and the northern boundary was dominated by a close-to-zero southerly wind (not shown). This resulted in a strong convergence within A2 (Figure 4f), which produced strong cyclonic vorticity (Figure 4e), contributing to induce more SWVs. This was the key reason for the abnormally active SWVs in the 2020 MYS.

6. Conclusion and Discussion

This study provided the first report on the historical rankings of the accumulated precipitation within different regions of the YRB during the extreme 1954, 1998, and 2020 MYSs. This was crucial to determine the most notable features for these extreme MYSs and to clarify their fundamental differences. It was shown that, the most notable features of the 2020 MYS lay in the area-averaged precipitation within A2-A4, and the maximum precipitation within A4. This differed from the extreme MYSs of 1954 and 1998 significantly, as the former was both notable for its averaged and maximum precipitation, whereas the latter was more notable for its maximum rainfall.

For the first time, quantitative contributions of the mesoscale vortices to the precipitation of extreme MYSs were shown. It was found that, vortices played a really important role in the extreme MYSs: for SWVs, they accounted for up to 50% of the total duration of the 2020 MYS, and induce up to 90% of its total precipitation in the Sichuan Basin. For DBVs, although they only accounted for less than 20% of the total durations of the extreme MYSs, their associated precipitation could reach up to above 1200 mm within A3 and above 1,500 mm within A4, which

Figure 4. Panel (a) illustrates the proportion (shading dots; %) of SWV-affected precipitation to the accumulated precipitation in the 1998 Mei-yu season (MYS). Panel (b) is the same as (a) but for DBV. Panel (c) is the same as (a) but for 2020, and panel (d) is the same as (b) but for 2020. Panel (e) shows the 42-year (from 1979 to 2020) time series of the A2-averaged MYS mean vorticity (solid red line, with dashed red line illustrating its trend; 10^{-6} s^{-1}), and the SWVs' (with a life span ≥6 hr) numbers (solid blue line, with dashed blue line illustrating its trend) from 2000 to 2013. Blue pentagrams with numbers mark SWVs' numbers in 1998 and 2020. Panel (f) shows the 42-year (from 1979 to 2020) time series of the A2-averaged MYS mean divergence (solid red line, with dashed red line illustrating its trend; 10^{-7} s^{-1}), and the meridional wind difference of $v_n - v_s$ (where v_n is the MYS mean of the averaged meridional wind along the northern boundary line of A2, and v_s is the MYS mean of the averaged meridional wind along the southern boundary line of A2; solid blue line, with dashed blue line illustrating its trend; m s^{-1}). Purple pentagrams mark the values of 1998 and 2020.

was ~40% or above of the total MYS precipitation. Therefore, accurate forecasts of vortices' activities were of great importance to improve the prediction of the MYS rainfall.

One of the most notable features of the extreme 2020 MYS was that, its averaged precipitation within A2 was the largest during the 70-year period from 1951 to 2020. The abnormally active SWVs were the key reason for the abnormally excessive precipitation within this region. It should be noted that, within A2, the divergence showed an increasing trend during the 42-year period from 1979 to 2020, which resulted in a decreasing trend of cyclonic vorticity. This means that conditions generally became more unfavorable for the SWVs' formation/maintenance during the 70-year period. However, in the 2020 MYS, a strong convergence, that was opposite to the increasing trend of the A2-averaged divergence appeared. It was mainly due to a strong southerly wind on the southern boundary of A2 and a close-to-zero southerly wind on the northern boundary. This produced strong cyclonic-vorticity through the vertical stretching within A2, which explained the abnormally active SWVs in the 2020 MYS. As the meridional wind is closely related to the summer monsoon, we suggest to conduct detailed studies on their relationships, which will further the understanding of extreme MYSs. In order to explore whether the MYS precipitation showed close relationships to the El Niño-Southern Oscillation (ENSO) and PDO (Pacific Decadal Oscillation), we calculated the linear correlation coefficients among them (Table S1 and Figure S4 in Supporting Information S1). It can be found that, there was a significant linear correlation between the A2-averaged precipitation and the PDO index, whereas, other correlations were not significant. This means that, for A2, its precipitation during the MYS showed a notable linear relationship to the PDO. Thus, we suggest to investigate the mechanisms underlying this relationship, which will be useful to improve the long-term prediction of the MYS precipitation within A2.

Data Availability Statement

The daily and hourly precipitation observation at meteorological stations from the China Meteorological Administration are available at http://data.cma.cn/en/?r=data/index&cid=9e5e973ce269a309. The ERA5 reanalysis data is downloaded from https://cds.climate.copernicus.eu/cdsapp#!/dataset/reanalysis-era5-pressure-levels?tab=form. The PDO index is downloaded from https://www.ncdc.noaa.gov/teleconnections/pdo/; and the ENSO index is downloaded from https://psl.noaa.gov/data/correlation/nina34.data.

Acknowledgments
This research was supported by the National Natural Science Foundation of China (Grant No. U2142202), the Strategic Priority Research Program of the Chinese Academy of Sciences (Grant No. XDA23090101), the National Natural Science Foundation of China (Grant Nos. 42075002; 41775046) and the Beijing Natural Science Foundation (Grant No. 8204072).

References

Bett, P. E., Martin, G. M., Dunstone, N., Scaife, A. A., Thornton, H. E., & Li, C. F. (2021). Seasonal rainfall forecasts for the Yangtze River basin in the extreme summer of 2020. *Advances in Atmospheric Sciences*, *38*, 2212–2220. https://doi.org/10.1007/s00376-021-1087-x

Chen, X., Dai, A., Wen, Z., & Song, Y. (2021). Contributions of Arctic sea-ice loss and East Siberian atmospheric blocking to 2020 record-breaking Meiyu-Baiu rainfall. *Geophysical Research Letters*, *48*, 10. https://doi.org/10.1029/2021GL092748

Clark, R. T., Wu, P., Zhang, L., & Li, C. (2021). The anomalous Mei-yu rainfall of summer 2020 from a circulation clustering perspective: Current and possible future prevalence. *Advances in Atmospheric Sciences*, *38*, 2010–2022. https://doi.org/10.1007/s00376-021-1086-y

Curio, J., Schiemann, R., Hodges, K.-I., & Turner, A.-G. (2019). Climatology of Tibetan Plateau vortices in reanalysis data and a high-resolution global climate model. *Journal of Climate*, *32*, 1933–1950. https://doi.org/10.1175/jcli-d-18-0021.1

Ding, Y., Liu, Y., & Hu, Z. (2021). The record-breaking Meiyu in 2020 and associated atmospheric circulation and tropical SST anomalies. *Advances in Atmospheric Sciences*, *38*, 1980–1993. https://doi.org/10.1007/s00376-021-0361-2

Dong, P.-M., & Zhao, S.-X. (2004). A diagnostic study of mesoscale lows (disturbances) on Meiyu front and associated heavy rainfall. *Chinese Journal of Atmospheric Sciences*, *28*(6), 876–891. https://doi.org/10.3878/j.issn.1006-9895.2004.06.07

Fu, S.-M., Li, W.-L., Sun, J.-H., Zhang, J.-P., & Zhang, Y.-C. (2015). Universal evolution mechanisms and energy conversion characteristics of long-lived mesoscale vortices over the Sichuan Basin. *Atmospheric Science Letters*, *16*, 127–134. https://doi.org/10.1002/asl2.533

Fu, S.-M., Liu, R.-X., & Sun, J.-H. (2018). On the scale interactions that dominate the maintenance of a persistent heavy rainfall event: A piecewise energy analysis. *Journal of the Atmospheric Sciences*, *75*, 907–925. https://doi.org/10.1175/JAS-D-17-0294.1

Fu, S. M., Sun, J. H., Luo, Y. L., & Zhang, Y. C. (2017). Formation of long-lived summertime mesoscale vortices over central east China: Semi-idealized simulations based on a 14-year vortex statistic. *Journal of the Atmospheric Sciences*, *74*, 3955–3979. https://doi.org/10.1175/jas-d-16-0328.1

Fu, S.-M., Yu, F., Wang, D.-H., & Xia, R.-D. (2013). A comparison of two kinds of eastward-moving mesoscale vortices during the Mei-yu period of 2010. *Science China Earth Sciences*, *56*(2), 282–300. https://doi.org/10.1007/s11430-012-4420-5

Fu, S.-M., Zhang, J.-P., Sun, J.-H., & Zhao, T.-B. (2016). Composite analysis of long-lived mesoscale vortices over the middle reaches of the Yangtze River valley: Octant features and evolution mechanisms. *Journal of Climate*, *29*, 761–781. https://doi.org/10.1175/JCLI-D-15-0175.1

Fu, S.-M., Zhang, J.-P., Tang, H., Jiang, L.-Z., & Sun, J.-H. (2020). A new mesoscale-vortex identification metric: Restricted vorticity and its application. *Environmental Research Letters*, *15*(12), 124053. https://doi.org/10.1088/1748-9326/abcac6

Hersbach, H., Bell, B., Berrisford, P., Hirahara, S., Horányi, A., Muñoz-Sabater, J., et al. (2020). The ERA5 global reanalysis. *Quarterly Journal of the Royal Meteorological Society*, *146*, 1999–2049. https://doi.org/10.1002/qj.3803

Japan Meteorological Agency. (2020). *Climate characteristics of record-heavy rain and record-low sunshine durations in Japan in July 2020*. Japan Meteorological Agency. Retrieved from http://ds.data.jma.go.jp/tcc/tcc/news/press_20200916.pdf

Kirk, J.-R. (2003). Comparing the dynamical development of two mesoscale convective vortices[J]. *Monthly Weather Review*, *131*(5), 862–890. https://doi.org/10.1175/1520-0493(2003)131<0862:ctddot>2.0.co;2

Liu, L., Wang, X., Feng, G., Dogar, M. M., Zhang, F., Zhiqiang, G., & Zhou, B. (2021). Variation of main rainy-season precipitation in eastern China and relevance to regional warming. *International Journal of Climatology*, *41*(3), 1767–1783. https://doi.org/10.1002/joc.6929

Lu, B., & Takaya, Y. (2021). Record Meiyu-Baiu of 2020: Reflections for prediction. *Science Bulletin*, *66*(19), 1939–1941. https://doi.org/10.1016/j.scib.2021.05.011

Ninomiya, K. (2000). Large-and meso-alpha-scale characteristics of Meiyu/Baiu front associated with intense rainfalls in 1–10 July 1991. *Journal of the Meteorological Society of Japan*, *78*(2), 141–157. https://doi.org/10.2151/jmsj1965.78.2_141

Oh, J. H., Kwon, W.-T., & Ryoo, S.-B. (1997). Review of the researches on Changma and future observational study (kormex). *Advances in Atmospheric Sciences*, *14*(2), 207–222. https://doi.org/10.1007/s00376-997-0020-2

Orlanski, I. (1975). A rational subdivision of scales for atmospheric processes. *Bulletin of the American Meteorological Society*, *56*, 527–530.

Park, C., Son, S., Kim, H., Ham, Y., Kim, J., Cha, D., et al. (2021). Record-breaking summer rainfall in South Korea in 2020: Synoptic characteristics and the role of large-scale circulations. *Monthly Weather Review*, *149*, 3085–3100. https://doi.org/10.1175/MWR-D-21-0051.1

Qiao, S., Chen, D., Wang, B., Cheung, H., Liu, F., Cheng, J., et al. (2021). The longest 2020 Meiyu season over the past 60 years: Subseasonal perspective and its predictions. *Geophysical Research Letters*, *48*, 9. https://doi.org/10.1029/2021GL093596

Song, L. C. (2018). *Yearbook of meteorological disasters in China* (p. 229). China Meteorological Press.

Sun, J.-H., & Zhao, S.-X. (2003). A study of special circulation during Meiyu season of the Yangtze River Basin in 1998. *Climatic and Environmental Research*, *8*(3), 291–306. https://doi.org/10.3878/j.issn.1006-9585.2003.03.04

Tanaka, M. (1992). Intraseasonal oscillation and the onset and retreat dates of the summer monsoon over east, Southeast Asia and the Western Pacific region using GMS high cloud amount data. *Journal of the Meteorological Society of Japan Series II*, *70*(1B), 613–629. https://doi.org/10.2151/jmsj1965.70.1B_613

Tao, S., & Chen, L. (1987). A review of recent research of the east Asian summer monsoon in China. In C.-P. Chang, & T. N. Krishnamurti (Eds.), *Monsoon meteorology* (pp. 60–92). Oxford University Press.

Tao, S. Y. (1980). *Rainstorms in China* (p. 225). Science Press. (in Chinese).

Volonté, A., Muetzelfeldt, M., Schiemann, R., Turner, A. G., & Klingaman, N. (2021). Magnitude, scale, and dynamics of the 2020 mei-yu rains and floods over China. *Advances in Atmospheric Sciences*, *38*. https://doi.org/10.1007/s00376-021-1085-z

Wang, L., Sun, X., Yang, X., Tao, L., & Zhang, Z. (2021). Contribution of water vapor to the record-breaking extreme Meiyu rainfall along the Yangtze River valley in 2020. *Journal of Meteorological Research*, *35*, 557–570. https://doi.org/10.1007/s13351-021-1030-1

Wei, K., Ouyang, C., Duan, H., Li, Y., & Zhou, S. (2020). Reflections on the catastrophic 2020 Yangtze River Basin flooding in southern China. *The Innovation*, *1*(2), 100038. https://doi.org/10.1016/j.xinn.2020.100038

Ye, Y., & Qian, C. (2021). Conditional attribution of climate change and atmospheric circulation contributing to the record-breaking precipitation and temperature event of summer 2020 in southern China. *Environmental Research Letters*, *16*, 044058. https://doi.org/10.1088/1748-9326/abeeaf

Zhang, J. P., Fu, S. M., Sun, J. H., Shen, X. Y., & Zhang, Y. C. (2015). A statistical and compositional study on the two types of mesoscale vortices over the Yangtze River Basin. *Climatic and Environmental Research*, *20*, 319–336.

Zhang, X.-L., Tao, S.-Y., & Zhang, S.-L. (2004). Three types of heavy rainstorms associated with the Meiyu front. *Chinese Journal of Atmospheric Sciences*, *28*(2), 187–205. https://doi.org/10.3878/j.issn.1006-9895.2004.02.03

Zhao, N., Manda, A., Guo, X., Kikuchi, K., Nasuno, T., Nakano, M., et al. (2021). A Lagrangian view of moisture transport related to the heavy rainfall of July 2020 in Japan: Importance of the moistening over the subtropical regions. *Geophysical Research Letters*, *48*, 5. https://doi.org/10.1029/2020GL091441

Zhao, S. X., Tao, Z.-Y., Sun, J. H., & Bei, N. F. (2004). *Study on mechanism of formation and development of heavy rainfalls on Meiyu front in Yangtze River* (p. 282). China Meteorological Press.

Zong, Y. Q., & Chen, X. Q. (2000). The 1998 flood on the Yangtze, China. *Natural Hazards*, *22*, 165–184. https://doi.org/10.1023/A:1008119805106